  Bull. Chem. Soc. Jpn., 62, 993—998 (1989)

A Least-Squares Method for Computing Rate Constants of Reversible, First-Order, Triangular Network Reactions and Its Application to the Intermolecular Rearrangements of Acetylacetonatobis(4,4,4-trifluoro-1-phenyl-1,3-butanedionato)ruthenium(III)

Yoshimasa HOSHINO, Ryouta TAKAHASHI, Kunio SHIMIZU, Gen P. SATÔ,* and Koichi AOKI†
Department of Chemistry, Faculty of Science, Sophia University, Kioicho, Chiyoda-ku, Tokyo 102
†Department of Electronic Chemistry, Graduate School at Nagatsuta, Tokyo Institute of Technology, Midori-ku, Yokohama 227
(Received August 31, 1988)

A useful method for computing the rate constants of reversible, first-order, triangular network reactions ($\mathbf{B}_1 \rightleftarrows \mathbf{B}_2$, $\mathbf{B}_2 \rightleftarrows \mathbf{B}_3$, $\mathbf{B}_3 \rightleftarrows \mathbf{B}_1$) is developed. It gives the best-fit set of the rate constants from the experimental data of the equilibrium constants and the mole fraction-time curves through an iterative least-squares method. This type of reaction can be classified into three categories for different shapes of the mole fraction-time curves. The method was successfully applied to determining the rate constants of the rearrangement reactions among the three isomers of [Ru(acac)(tfpb)$_2$] (acac$^-$=acetylacetonate ion, tfpb$^-$=4,4,4-trifluoro-1-phenyl-1,3-butanedionate ion) in *N,N*-dimethylformamide at 90 °C. The direct conversion between the *de,fc*-bis(tfpb) isomer and the *cf,ed*-bis(tfpb) isomer was forbidden. The twist mechanisms are incompatible with this fact.

The simplest network reaction is a first-order reversible reaction of three components with a triangular scheme, exemplified by isomerization of butene[1] and cobalt complexes.[2,3] A theory of the triangular network reaction has been fully developed by Wei and Prater.[1] Numerical methods for determining rate constants have been presented in a detailed review.[4] Since the differential equations for the kinetics is linear, the solution is composed of a sum of exponential terms.[5] In order to evaluate rate constants from experimental data through combinations of exponential functions, it is necessary to linearize the equation. The numerical method of Wei and Prater[1] is essentially based on the linearization around the equilibrium. Consequently, a number of accurate data points near the equilibrium are required for the determination of rate constants. Such data are difficult to obtain when the experimental precision is limited by the presence of side reactions or for other reasons; besides, a sufficient number of such data are rarely available if the reaction is very slow. Furthermore, this numerical method does not give the absolute values of the rate constants, but only their ratios. It is desirable to explore a technique that gives the absolute values of rate constants making use of all the experimental points.

This report is devoted to development of a numerical technique based on nonlinear regression and to the evaluation of the rate constants of the triangular network of a set of the isomers of β-diketonato-ruthenium(III) complexes.

Theoretical

Figure 1 illustrates the reaction scheme of the triangular network, where k_{ij} is the rate constant of the reaction $\mathbf{B}_i \rightarrow \mathbf{B}_j$. We denote the mole fraction of species $\mathbf{B}_j$ by x_j. Then kinetic equations for the triangular reaction are

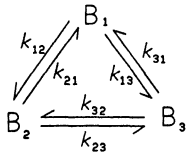

Fig. 1. Model of the triangular network reversible reaction. The equilibrium constants are defined in Eq. 5.

$$dx_1/dt = -(k_{12}+k_{13})x_1 + k_{21}x_2 + k_{31}x_3 \quad (1)$$
$$dx_2/dt = k_{12}x_1 - (k_{21}+k_{23})x_2 + k_{32}x_3 \quad (2)$$
$$dx_3/dt = k_{13}x_1 + k_{23}x_2 - (k_{31}+k_{32})x_3, \quad (3)$$

where t is the time since the beginning of the reaction. The initial conditions are given by

$$t=0: x_1=x_1^0,\ x_2=x_2^0,\ x_3=x_3^0. \quad (4)$$

Here x_j^0 is the initial mole fractions of species $\mathbf{B}_j$. We define the following three equilibrium constants:

$$K_{12}=x_2^e/x_1^e=k_{12}/k_{21}$$
$$K_{23}=x_3^e/x_2^e=k_{23}/k_{32} \quad (5)$$
$$K_{31}=x_1^e/x_3^e=k_{31}/k_{13}.$$

The superscript e means the equilibrium. An alternative form of Eq. 5 is

$$x_1^e=(1+K_{12}+1/K_{31})^{-1}$$
$$x_2^e=(1+K_{23}+1/K_{12})^{-1} \quad (6)$$
$$x_3^e=(1+K_{31}+1/K_{23})^{-1}.$$

Obviously only two of the three equilibrium constants are independent because $K_{12}K_{23}K_{31}=1$. Hence the following relation holds:

$$k_{12}k_{23}k_{31}=k_{13}k_{32}k_{21}, \quad (7)$$

The initial problem of Eqs. 1—4 can be solved by means of a conventional method, e.g., the Laplace transformation, although it is cumbersome to elim-

inate two of the three dependent variables. The solution is expressed by

$$x_j = x_j^e + r_j e^{-pt} + s_j e^{-qt}, \quad (j=1, 2, 3) \tag{8}$$

with

$$p = \{\alpha - (\alpha^2 - 4\beta)^{1/2}\}/2 \tag{9}$$

$$q = \{\alpha + (\alpha^2 - 4\beta)^{1/2}\}/2 \tag{10}$$

$$r_j = (x_j^0 p - \kappa_j + \lambda_j/p)/(p-q) \tag{11}$$

$$s_j = (x_j^0 q - \kappa_j + \lambda_j/q)/(q-p),$$

where

$$\kappa_1 = x_1^0(k_{21}+k_{23}+k_{32}+k_{31}) + x_2^0 k_{21} + x_3^0 k_{31} \tag{12a}$$

$$\kappa_2 = x_1^0 k_{12} + x_2^0(k_{12}+k_{13}+k_{31}+k_{32}) + x_3^0 k_{32} \tag{12b}$$

$$\kappa_3 = x_1^0 k_{13} + x_2^0 k_{23} + x_3^0(k_{12}+k_{21}+k_{23}+k_{13}) \tag{12c}$$

$$\lambda_1 = k_{31}k_{21} + k_{23}k_{31} + k_{32}k_{21} \tag{13a}$$

$$\lambda_2 = k_{12}k_{32} + k_{31}k_{12} + k_{13}k_{32} \tag{13b}$$

$$\lambda_3 = k_{23}k_{13} + k_{12}k_{23} + k_{21}k_{13} \tag{13c}$$

$$\alpha = k_{12}+k_{21}+k_{23}+k_{32}+k_{31}+k_{13} \tag{14}$$

$$\beta = k_{12}k_{23}/x_3^e + k_{23}k_{31}/x_1^e + k_{31}k_{12}/x_2^e. \tag{15}$$

A characteristic of Eq. 8 is that the arguments of the exponential are common to the three species. A set of these equations are essentially the same as Wei and Prater's matrix expression.[2]

Examples of the x_j-t curves calculated for the case where $K_{12}=K_{23}=K_{31}$, $x_1^0=1$, and $x_2^0=x_3^0=0$ are shown in Fig. 2. Here the three sets of the curves represent the following typecal cases:

(A) When the values of k_{ij} is comparative (the solid curves), x_2 and x_3 increase monotonically at the sacrifice of x_1 and then approach the equilibrium values. The rate of the decrease of x_1 is almost the same as the sum of the rates of the increase of x_2 and x_3. A special case is that all the values of k_{ij} are the same. Then Eq. 8 reduces to

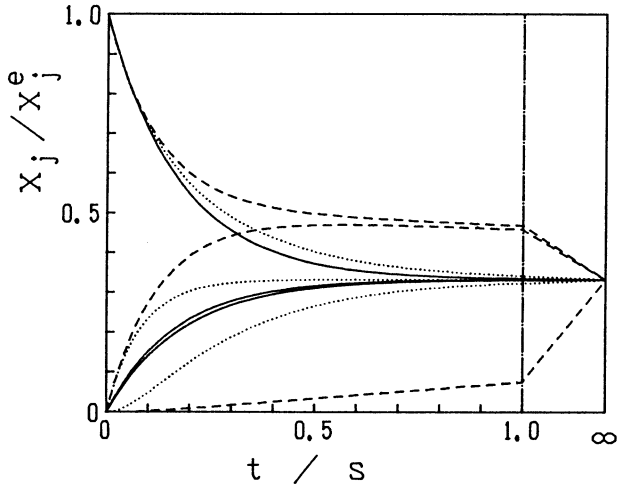

Fig. 2. Variations of x_j (j=1,2,3) with time at K_1=K_2=K_3=1 calculated from Eqs. 8—15 for (k_{12}, k_{23}, k_{31})=(2.0, 2.0, 1.8)(——), (4.0, 4.0, 0.0)(·····) and (4.0, 0.2, 0.0)(----). The initial conditions are x_1^0=1.0, x_2^0=0, and x_3^0=0.

$$x_j = 1/3 + (x_j^0 - 1/3)\exp[-3k_{ij}t]. \tag{16}$$

Then the overall relaxation time is $1/(3k_{ij})$.

(B) When both k_{12} and k_{23} are large and k_{31} is small (the dotted curves), $\mathbf{B_3}$ is generated through $\mathbf{B_2}$ without direct supply from $\mathbf{B_1}$. The increase of x_3 is slower than that of x_2. Since x_3 increases very slowly at the beginning, the curve for x_3 is a sigmoid. In an extreme case where $k_{31}=k_{13}=0$, the network reduces to a two-step consecutive reaction.

(C) When k_{12} is large and both k_{23} and k_{31} are small (the dashed curves), $\alpha^2 \gg 4\beta$ or $q \gg p$. Then the mole fractions vary mainly with $\exp(-\alpha t)$ or $\exp[-(k_{12}+k_{21})]$. In this case, x_1 and x_2 converge before reaching the equilibrium value.

Let us explore a technique of determining the rate constants from a set of experimental x_j curves. It is assumed that the equilibrium constants are known in advance. Then the unknown parameters are k_{12}, k_{23}, and k_{31}. It is possible to use any other three independent parameters composed of adequate combinations of k_{12}, k_{23}, and k_{31}: for example (α, β, κ_1) or (p, q, r_1). Choice of the independent parameters is important for successful curve fitting. We chose (p, q, r_1), because this set is directly connected with the shape of the x_j-t curves.

A convenient numerical technique of curve fitting is the least squares method.[6] Since Eq. 8 is nonlinear with respect to p, q, and r_1, it has to be linearized. The Taylor expansion of Eq. 8 is carried out around a set of tentative values of p', q', and r_j'. Retaining only the linear terms, one has

$$x_j = x_j^e + (x_j^0 - x_j^e)e^{-q't} - (e^{-p't} - e^{-q't})r_j + r_j' te^{-p't}(p-p') - (x_j^0 - x_j^e + r_j')te^{-q't}(q-q'). \tag{17}$$

The sum of squares of the differences between Eq. 17 and the experimental values for each x_j-t curve is $\sum(x_j - x_{jn})^2$, where x_{jn} is the value of x_j at the n-th experimental point. The minimum condition for the total sum of squares of a set of three x_j-t curves is give by Eq. 18 (note that the adjustable parameters are p, q, r_1, r_2, and r_3).

$$\sum_{j=1}^{3}[\partial\sum_n(x_j - x_{jn})^2/\partial p + \partial\sum_n(x_j - x_{jn})^2/\partial q + \partial\sum_n(x_j - x_{jn})^2/\partial r_j] = 0. \tag{18}$$

The values of p, q, r_1, r_2, and r_3 that minimize the total sum of squares for a given set of p', q', r_1', r_2', and r_3' are determined by solving Eq. 18. These values are inserted into Eq. 17 in place of p', q', r_1', r_2', and r_3'. By solving the resultant equation, a new set of p, q, r_1, r_2, and r_3 that gives a better fitting will be obtained. This procedure is repeated until the values of these parameters converge. The convergence naturally depends on how the values of the first set of p', q', r_1', r_2', and r_3' are close to the final values; too unrealistic initial values may result in divergence. A method of determining the initial values will be described in

Results and Discussion. Equation 18 is rewritten as

$$\mathrm{D}\begin{pmatrix} p \\ q \\ r_1 \\ r_2 \\ r_3 \end{pmatrix} = \mathrm{F}\begin{pmatrix} p' \\ q' \\ r_1' \\ r_2' \\ r_3' \end{pmatrix} \quad (19)$$

Here D is a symmetric square matrix with five columns. The element of D at the h-th column and the m-th line is given by $\sum_n \sum_j a_h a_m$ (j=1,2,3; h=1,2,···,5; m=1,2,···,5), where

$$\begin{aligned} a_1 &= -r_j' t_n \exp(-p' t_n) \\ a_2 &= -\{x_j^0 - x_j^e - r_j'\} t_n \exp(-q' t_n) \\ a_3 &= a_4 = a_5 = \exp(-p' t_n) - \exp(-q' t_n) \end{aligned} \quad (20)$$

and F is a diagonal matrix the element of which at the m-th column, b_m (m=1,2,···,5) is given by

$$b_m = \sum_{j=1}^{3} \sum_n [x_j^e + r_j' \exp(-p' t_n) - x_{jn} + \{x_j^0 - x_j^e - r_j'\} \exp(-q' t_n)] a_m. \quad (21)$$

Equation 19 is the simultaneous equation for p, q, r_1, r_2, and r_3. Its solution and the iteration can be executed on a personal computer. An example of estimation of the initial values of p', q', r_1', r_2', and r_3' is given below.

Experimental

Chemicals. The following three geometrical isomers of acetylacetonatobis(4,4,4-trifluoro-1-phenyl-1,3-butanedionato)ruthenium(III) were prepared and isolated according to the procedure described previously:[7] *ab*-acetylacetonato-*de*,*fc*-bis(4,4,4-trifluoro-1-phenyl-1,3-butanedionato)ruthenium(III) (**B**$_1$), *ab*-acetylacetonato-*cf*,*de*-bis(4,4,4-trifluoro-1-phenyl-1,3-butanedionato)ruthenium(III) (**B**$_2$), and *ab*-acetylacetonato-*cf*,*ed*-bis(4,4,4-trifluoro-1-phenyl-1,3-butanedionato)ruthenium(III) (**B**$_3$). Deionized water (Barnstead, NANOpure) was used, and the other solvents were of liquid-chromatographic grade unless otherwise stated.

Chromatography. High-pressure liquid chromatography was conducted on a Toyo Soda CCPM liquid chromatograph with a Toyo Soda UV-8000 ultraviolet-visible detector operating at 304 nm. The three isomers were separated on a silanised silica gel column (250 mm length, 4 mm internal diameter; Merck LiChrosorb RP-18, particle size 5 μm) by a mixture or methanol-water-acetonitrile (8:3:2 by volume) at a flow rate of 1 cm^3 min^{-1}. Retention time were 19 min for **B**$_3$, 20 min for **B**$_2$, and 23 min for **B**$_1$.

The peak area (defined as the product of the peak hight and the half-peak width) was proportional to the amount of each isomer. The mole fractions of the isomers in the reaction mixtures were determined by means of calibration curves drawn for a standard series of mixtures prepared gravimetrically from the isolated samples of the isomers.

Kinetic Measurement. Each of the isomers (**B**$_1$, 3.87×10^{-5} mol; **B**$_2$, 4.02×10^{-5} mol; **B**$_3$, 2.29×10^{-5} mol) was dissolved in 50 cm^3 of *N*,*N*-dimethylformamide (DMF) of the spectrophotometric grade (Dojindo Laboratories, Dotite Spectrosol). Forty five 0.1 cm^3 aliquots of each solution were transferred into glass tubes of 1.5 mm internal diameter. After the contents were deoxygenated by passing argon through a glass capillary for 1 min, the tubes were sealed in a flame and mounted on a holder. During these operations, the solutions were cooled with ice-water. The reaction was started by immersing the holder with 135 tubes into an oil bath (Thomas Kagaku Thermostatic Oil Bath, T-201) maintained at (90±0.1) °C. Three tubes, one for each starting isomer, were removed from the oil bath at certain time intervals and immediately quenched in ice-water. Each tube was then cut open, and a 2 mm^3 portion of its content was injected into the chromatograph.

The mole fractions of the three isomers under equilibrium conditions were determined in a similar manner when the reaction mixtures were allowed to stand at 90 °C until no further change was detected (2—3 days).

No indication of any side reactions was observed.

Results and Discussion

The three equilibrium constants are presented in Table 1. They were independent of the starting species and are not far from the statistical values (4:1:2).

Figures 3a, 3b, and 3c show variations of x_j with the time when starting species are **B**$_1$, **B**$_2$, and **B**$_3$, respectively. Evidently, the reactions **B**$_1$→**B**$_3$ and **B**$_3$→**B**$_1$ are slower than the other reactions, and the reaction **B**$_2$→**B**$_3$ is slower than the reaction **B**$_2$→**B**$_1$. The curves in Fig. 3a are essentially similar to the dotted curves in Fig. 2, suggesting that the reaction belongs to case (B).

The initial values of parameters p', q', r_1', r_2', and r_3' were determined as follows. If $q \gg p$, plot of $\ln(x_{jn} - x_j^e)$ against t_n at long times should fall on a straight line, of which slope and intercept give approximate values of p and r_j, respectively. The plots for the three curves with x_j^0=1 in Figs. 3a, 3b, and 3c are straight lines (Fig. 4), although their slopes are not quite the same. We took the slope of the line corresponding to Fig. 3a (circles in Fig. 4) as the initial value of p' and its intercepts as the initial value of r_1'. The initial value of q' was set to be twice the initial value of p' and $r_2' = r_3' = 0$ (there was no particular reason for this choice). The values of p, q, r_1, r_2, r_3 for the data of Fig. 3a were successfully determined by inserting these initial values into Eqs. 19—21 and executing the iteration.

The same procedure was applied to the data of Figs. 3b and 3c. Values of the five parameters thus obtained are listed in Table 2. From these values, three sets of κ_j were calculated by means of the following equation:

Table 1. Equilibrium Constants[a]

Starting species	$K_{12}=x_2^e/x_1^e$	$K_{23}=x_3^e/x_2^e$	$K_{31}=x_1^e/x_3^e$	Number of runs
B$_1$	1.820 (0.059)	0.677 (0.018)	0.813 (0.014)	3
B$_2$	1.799 (0.086)	0.665 (0.044)	0.839 (0.037)	4
B$_3$	1.823 (0.054)	0.694 (0.044)	0.792 (0.027)	2
Average	1.811 (0.064)	0.675 (0.034)	0.820 (0.032)	

a) Values in the parentheses are standard deviations.

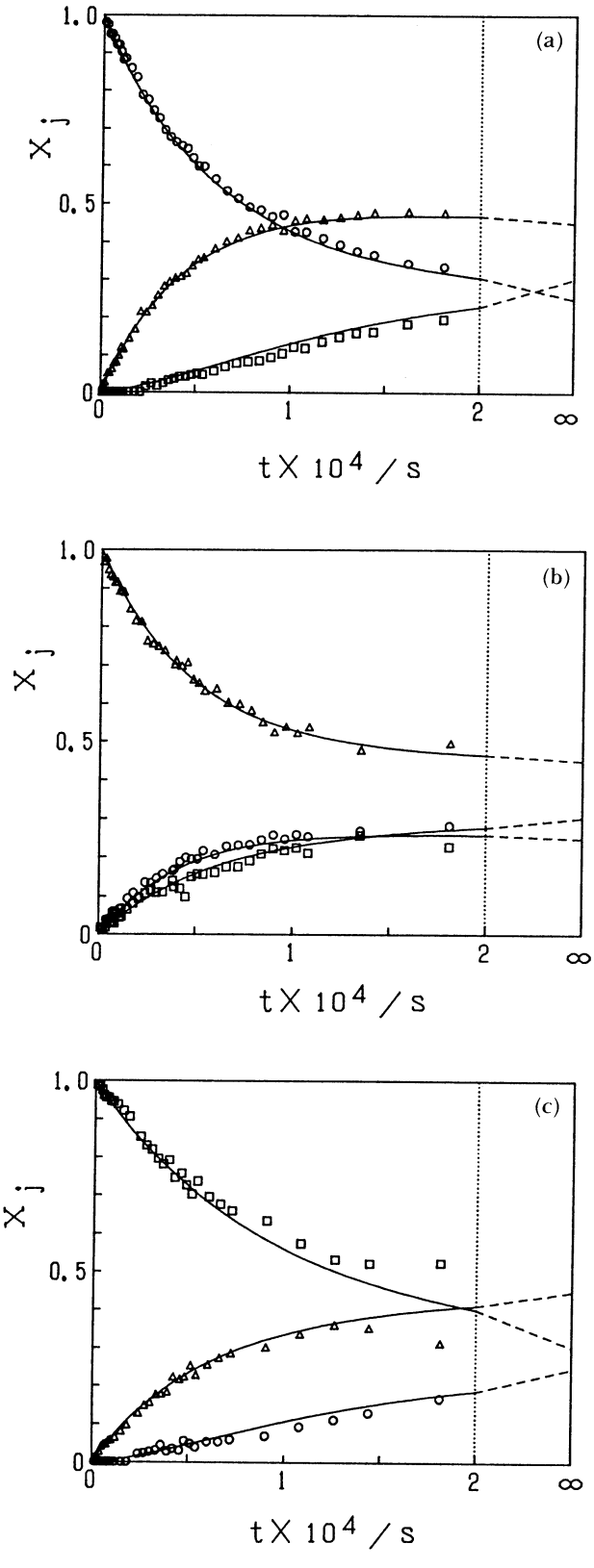

Fig. 3. Variations of mole fractions, x_j (j=1,2,3), for $\mathbf{B}_1$(○), $\mathbf{B}_2$(△), and $\mathbf{B}_3$(□) with time. Starting species are $\mathbf{B}_1$(a), $\mathbf{B}_2$(b), and $\mathbf{B}_3$(c). Solid lines are simulated curves calculated from Eqs. 8—15 at the following values: K_{12}=1.811, K_{23}=0.675, K_{31}=0.820, k_{12}=1.228×10^{-4} s^{-1}, k_{23}=0.476×10^{-4} s^{-1}, and k_{31}=0.027×10^{-4} s^{-1}.

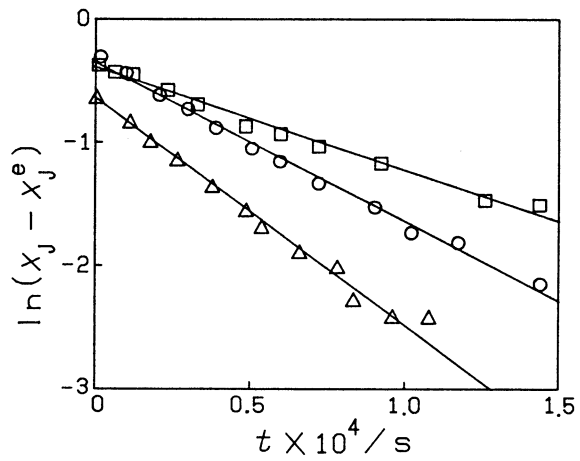

Fig. 4. Logarithmic plots of deviation of the mole fraction from the equilibrium against the time. Symbols ○, △, and □ correspond respectively to data ○ in Fig. 3a, data △ in Fig. 3b, and data □ in Fig. 3c.

Table 2. Auxiliary Kinetic Parameters Required for Determination of k_{ij}

Starting species	p×10^4 / s^{-1}	q×10^4 / s^{-1}	r_1	r_2	r_3
$\mathbf{B}_1$	0.863	2.116	0.333	0.177	−0.510
$\mathbf{B}_2$	0.681	2.266	0.078	0.066	−0.144
$\mathbf{B}_3$	0.584	2.875	−0.286	−0.236	0.522

Table 3. Linearly Combined Rate Constants, κ_j

Starting species	κ_1×10^4 / s^{-1}	κ_2×10^4 / s^{-1}	κ_3×10^4 / s^{-1}
$\mathbf{B}_1$	1.805	1.171	0.002
$\mathbf{B}_2$	0.685	1.803	0.459
$\mathbf{B}_3$	0.058	0.750	2.650

$$\kappa_j = x_j^0(p+q) - pr_j - q(x_j^0 - x_j^e - r_j), \qquad (22)$$

which has been derived from Eq. 11 by eliminating λ_j. The values of κ_j are listed in Table 3. Since κ_j is the linear combinations of k_{12}, k_{23}, and k_{31} (Eq. 12), the rate constants can be immediately estimated: κ_2 for $\mathbf{B}_1$ (1.2×10^{-4} s^{-1}) is $x_1^0 k_{12}$, while κ_1 for $\mathbf{B}_2$ (0.68×10^{-4} s^{-1}) is $x_2^0 k_{21}$, and so forth. However, the k values obtained in this way are not consistent. For example, the calculated values of k_{12} and k_{21} do not satisfy k_{12}/k_{21}=1.811 (=K_{12}). There are nine known values for κ_j from which three k's are to be determined. This redundancy can be effectively utilized for increasing the precision of the computation in the following way.

Let us consider a three-dimensional space (k_{12}, k_{23}, k_{31}). Each κ_j value is represented as a plane in this space. The most probable values of k_{12}, k_{23}, and k_{31} will be given by the coordinates of the center of the polyhedron defined by the nine κ_j planes. The center is the point where the total sum of squares of the distances between that point and the nine planes is a

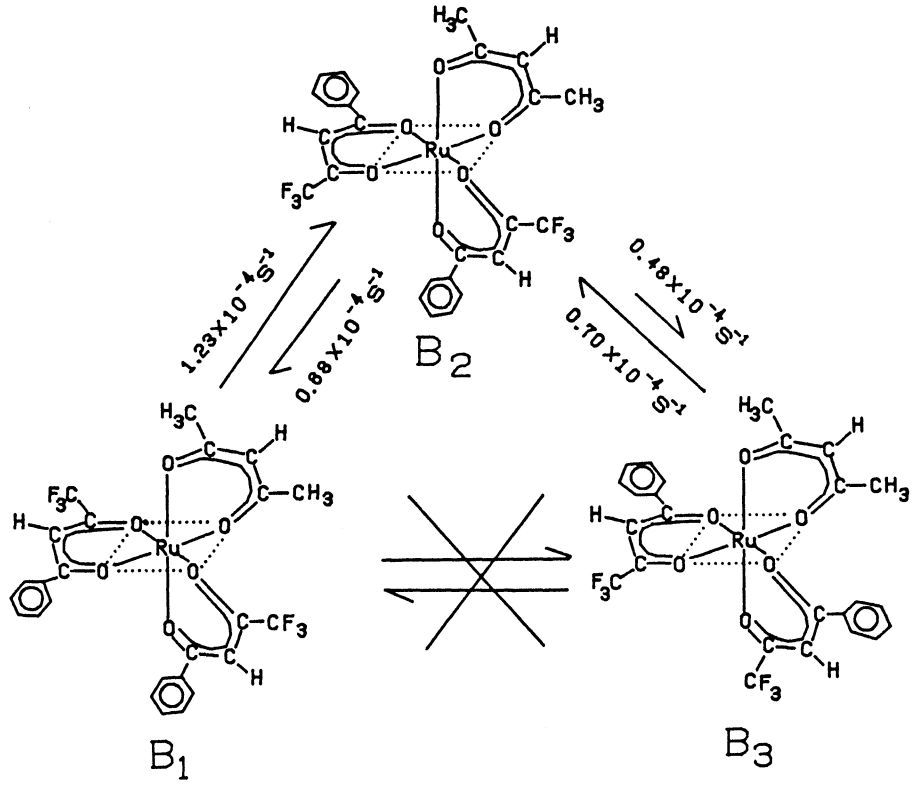

Fig. 5. Kinetic parameters for the isomerization of [Ru(acac)(tfpb)].

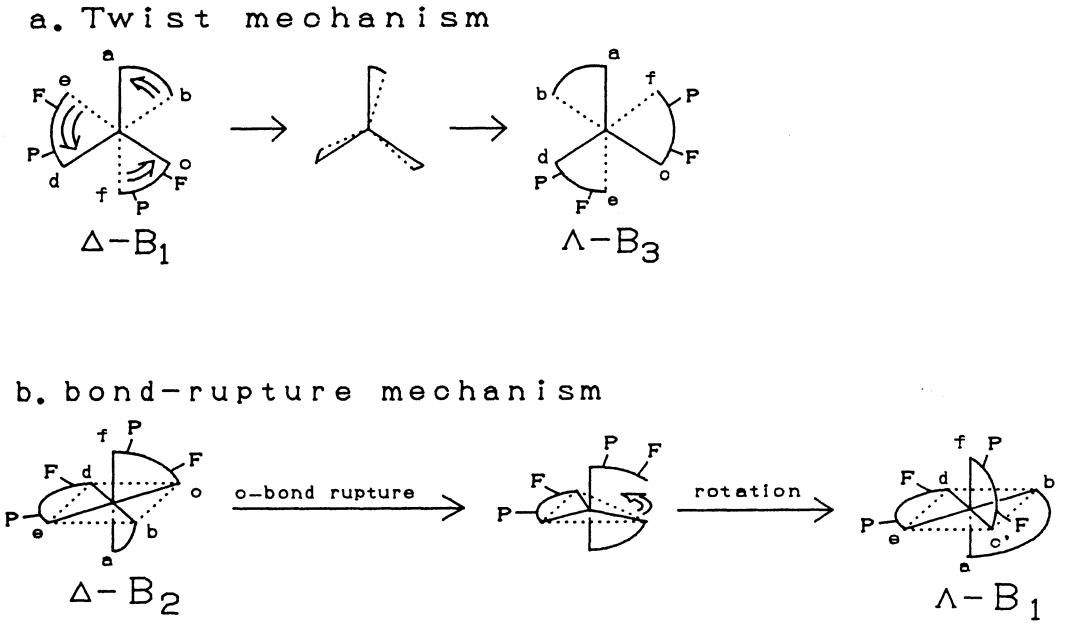

Fig. 6. Examples of twist mechanism (a) and bond-rupture mechanism (b).

minimum. This least squares method leads to the following values: $k_{12}=1.22_8\times10^{-4}$ s^{-1}, $k_{23}=0.47_6\times10^{-4}$ s^{-1}, and $k_{31}=0.02_7\times10^{-4}$ s^{-1}. The standard deviation is $0.05_3\times10^{-4}$ s^{-1}. The curves in Fig. 3 are calculated from Eq. 8 with these k values. They are in good agreement with the experimental data. The deviation of the points from the calculated curves for $t>$ca. 1.5×10^4 s is attributable to experimental errors. Noteworthy is the fact that the direct conversion between **B**$_1$ and **B**$_3$ was forbidden. Isomerization reactions of octahedral tris-chelate complexes are generally interpreted in terms of two basic pathways: twist mechanisms and bond-rupture mechanisms.[8] The twist mechanisms are not compatible with this fact because

the rotation around two of the possible four axes allows the conversion between $\mathbf{B}_1$ and $\mathbf{B}_3$ (for example, Fig. 6a). On the contrary, certain types of bond-rupture pathways[9] (for example, Fig. 6b) are in accord with the absence of the direct conversion between $\mathbf{B}_1$ and $\mathbf{B}_3$. More detailed discussion will be presented in a subsequent paper.

The technique of determining the rate constants presented above has the following advantages: 1) absolute values of the rate constants can be obtained; 2) all the experimental points, not only those near the equilibrium, are effectively utilized; 3) the rate constants are determined consistently from all the available data; 4) the requirement of the precision of the data is not too strict.

The authors' thanks are due to Dr. S. F. Howell, Sophia University, for correcting the manuscript.

References

1) J. Wei and C. D. Prater, "Advances in Catalysis," Academic Press Inc., New York (1962), Vol. 13.

2) M. Watabe, S. Kawaai, and S. Yoshikawa, *Bull. Chem. Soc. Jpn.*, **49**, 1845 (1976).

3) M. Watabe, M. Zama, and S. Yoshikawa, *Bull. Chem. Soc. Jpn.*, **51**, 1354 (1978).

4) M. Boudart, "Kinetics of Chemical Processes," Prentice-Hall Inc., Englewood Cliffs, New Jersey (1968).

5) F. H. Raven, "Mathematics of Engeneering Systems," McGraw-Hill, New York (1966), Chap. 3.

6) S. L. S. Jacoby, J. S. Kowalik, and J. T. Pizzo, "Iterative Methods for Nonlinear Optimization Problems," Prentice-Hall Inc., Englewood Cliffs, New Jersey (1972).

7) Y. Hoshino, Y. Yukawa, A. Endo, K. Shimizu, and G. P. Satô, *Chem. Lett.*, **1987**, 845.

8) J. G. Gordon, II, and R. H. Holm, *J. Am. Chem. Soc.*, **92**, 5319 (1970).

9) E. L. Muetterties, *J. Am. Chem. Soc.*, **90**, 5097 (1968).